OpenNano 1 (2016) 25–35

Contents lists available at ScienceDirect

OpenNano

journal homepage: www.elsevier.com/locate/onano

Modeling of the controlled release of betacarotene into anhydrous ethanol from microcapsules

Jucelio Kilinski Tavares [a,*], Antônio Augusto Ulson de Souza [a], José Vladimir de Oliveira [a], Wagner Luiz Priamo [b], Selene M.A. Guelli Ulson de Souza [a]

[a] Chemical and Food Engineering Department, Federal University of Santa Catarina, PO Box 476 - Campus Universitário, Zip Code 88.040-900 Florianópolis, SC, Brazil

[b] Laboratory of Separation Processes, Federal Institute of Education, Science and Technology of Rio Grande do Sul State - IFRS - Campus Sertão, Rodovia RS 135, Km 25 - Distrito Eng. Luiz Englert - Caixa Postal 21, CEP 99170-000, Sertão, RS, Brazil

ARTICLE INFO

Article history:
Received 3 May 2016
Received in revised form
25 May 2016
Accepted 26 May 2016
Available online 3 June 2016

Keywords:
Controlled release
Microcapsules
Modeling
Active principles
Simulation

ABSTRACT

In this paper several models of the mass transfer process are described with the aim of simulating the release of active principles from matrix-type polymeric microcapsules. The following mathematical models, which are available in the literature, are applied in this study: Fick's second law (CDMASSA), the linear drive force (LDF), an analytical model and other semi-empirical models. The release of the active principle (betacarotene) contained in microcapsules (PHBV) into a solvent (ethanol) was investigated. It was observed that the model obtained with Fick's second law provided a better fit with the literature data compared with the LDF model, the analytical model and the semi-empirical models. It can be concluded from this finding that the most complete model, based on the phenomenology of the problem, provided the best result.

1. Introduction

The mathematical modeling of the controlled release of active agents present in micro- and nanometric-scale particles is of great relevance in relation to predicting the behavior of dosing systems for drugs, agrotoxic chemicals, cosmetic products, aromas and other products. A series of mathematical models is currently used to explain the processes involved in the controlled release of active principles, based on biodegradable polymeric release systems [1]. In these models, the mass transfer parameters are required in order for the models to adequately represent the mechanisms associated with the release of the molecules of the active principles. The mathematical modeling of the release allows a better understanding of the strategies used for the retention of the active principles in a polymeric structure, as well as control over their release.

The study of the mechanisms associated with the release of encapsulated products is a fundamental stage in predicting the behavior of these particles when used in a commercial application. The modeling of these mechanisms is associated

Abbreviations: Energy, Unit of energy; L, Unit of spatial dimension; LDF, Linear Drive Force; M, Unit of mass; PHBV, Poly (3-hydroxybutyrate-co-3-hydroxyvalerate); t, Unit of time; T, Unit of temperature; -, Adimensional.

* Corresponding author.
E-mail addresses: helionx@yahoo.com.br (J.K. Tavares), augusto@enq.ufsc.br (A.A.U. de Souza), vladimir@enq.ufsc.br (J.V. de Oliveira), wagner.priamo@sertao.ifrs.edu.br (W.L. Priamo), selene.souza@ufsc.br (S.M.A.G.U. de Souza).

http://dx.doi.org/10.1016/j.onano.2016.05.001

Nomenclature

a	Constant which incorporates the structural and geometric characteristics of the active principle (Equation 15) [-/t^n]
A	Parameter which contributes to the burst effect (Equation 15) [-]
B	Parameter which contributes to the continuous release phase (Equation 15) [-]
C	Mass concentration of solute [M/L^3]
$\mathbf{C_A}$	Molar concentration of species A [mol/L^{-3}]
$\mathbf{C_A^*}$	Molar concentration of species A at equilibrium [mol/L^{-3}]
$\boldsymbol{C_{Al}}$	Molar concentration of species A in liquid phase [mol/L^{-3}]
$\boldsymbol{C_{ARp}}$	Molar concentration of species A in radius Rp [mol/L^{-3}]
$\mathbf{C_{eq}}$	Mass concentration at equilibrium [M/L^3]
$\mathbf{C_l}$	Mass concentration of liquid phase [M/L^3] (Figure 1)
$\mathbf{C_{ms}}$	Solubility of active substance in the matrix [M/L^3]
$\hat{\mathbf{C}}_\mathbf{p}$	Calorific capacity [energia/T]
$\mathbf{C_S}$	Mass concentration of solid phase [M/L^3] (Figure 1)
$\mathbf{C_0}$	Initial mass concentration of the active principle in the particle [M/L^3]
$\mathbf{D_{AB}}$	Mass diffusivity of solute A in medium B [L^2/t]
$\mathbf{D_{ABWC}}$	Diffusivity of solute A in medium B of the Wilke-Chang model [L^2/t]
$\boldsymbol{D_{AP}}$	Diffusivity of solute A in the polymer [L^2/t]
$\mathbf{D_m}$	Mass diffusivity [L^2/t]
$\mathbf{D_{pol}}$	Diffusivity of active principle in the polymer [L^2/t]
Diam	Diameter of the sphere [L]
F	F number of the statistical *F* test [-]
$\mathbf{k_B}$	Boltzmann constant [L^2.M/t^2.T]
$\mathbf{k_{m2}}$	Mass transfer coefficient [L/t]
K	Constant of proportionality [M/t]
Kp	Partition coefficient [-]
$\boldsymbol{M_B}$	Molar mass of B [M/mol]
n	Release exponent [-]
q	Mass concentration in the solid phase [M/L^3]
r	Particle radius [L]
$\mathbf{r_0}$	Radius of the spherical matrix [L]
$\boldsymbol{r_A}$	Radium of molecule A [L]
R	Universal gas constant [Energy/mol.T]
$\mathbf{R_p}$	Particle Radius [L]
Re	Reynolds number [-]
Sch	Schmidt number [-]
t	Time [t]
T	Temperature [T]
$\boldsymbol{v_\infty}$	Velocity of the medium [L/t]
V	Volume of liquid [L^3]
$\boldsymbol{V_{bA}}$	Molecular volume of A [L^3/mol]
$\mathbf{V_i}$	Molecular volume of A or B [L^3/mol]
$\mathbf{V_S}$	Volume of solid phase [L^3]
$\mathbf{x_A}$	Molar fraction of A [-]

Greek letters

$\boldsymbol{\alpha}$	Kinetic rate constant [-/t]
$\boldsymbol{\beta}$	Kinetic rate constant [-/t]
$\boldsymbol{\delta_i}$	Solubility of A or B [M/L^3]
$\boldsymbol{\varepsilon}$	Porosity of the matrix [-]
$\boldsymbol{\mu_B}$	Dynamic viscosity [M/L.t]
$\boldsymbol{\rho}$	Density [M/L^3]
$\boldsymbol{\tau}$	Tortuosity factor of the capillary system [-]
$\boldsymbol{\gamma_A}$	Coefficient of activity of A [-]

with factors such as the properties of the products to be encapsulated (active principle), of the encapsulating agent and of the medium, which include the temperature, pH, salinity and composition. Along with these factors, the behavior of the particles is affected by their morphology, since they can have a liquid core and a solid shell, they can be a solid medium in which the active substance is distributed, or they can even be comprised of several cores.

The type of substance encapsulated, the polymorphic shape of the particle, the crystallinity, the particle size, the solubility and quantity of the product incorporated and the characteristics of the encapsulating and encapsulated agents can influence the release of the active principle.

When a polymeric structure is produced for the encapsulation and release of active substances the behavior of the system in relation to the release needs to be predicted. The release of the active principle in an appropriate manner needs to be ensured and the behavior of this release over time needs to be ascertained in order to guarantee the efficiency and the safety of the release into the medium [2–5]. Controlled-release systems are an efficient way to ensure the local release of drugs [6].

In this study, the release of betacarotene microencapsulated in poly-(3-hydroxybutyrate-co-3-hydroxyvalerate) (PHBV), a natural polyester obtained from micro-organisms, was investigated [7].

2. Materials and methods

2.1. Materials

The studied nanospheres were prepared from a PHBV with molar mass of 196.000 and polydispersity index of 1.85 (measured by GPC using a calibration curve obtained from polystyrene standards), was kindly supplied by the PHB Industrial

S. A. (Brazil). The solvent anhydrous ethanol from Merck (Germany), with purity greater than 99.0%, was used as received. The preparation procedure and characterization of nanospheres were described in of [7]. Four types of nanoparticles of varying drug content with same size, the mean diameter size particle was about 5.50×10^{-5} cm. The drug loadings varied from β-Carotene mass fraction 28–49% (w/w).

2.2. β-Carotene release in vitro

To determine the β-carotene release kinetics in the organic solvent, the system temperature and orbital motion were kept constant at 313.15 ± 0.5 K and 80 rpm, respectively. For the release experiments, four β-carotene concentrations into organic solution varying from 12 to 30 mg ml^{-1}, at a fixed PHBV concentration of 30 mg ml^{-1}. All tests were performed in 100 ml Erlenmeyers flasks, protected at the top with plastic wrap to prevent solvent evaporation, incubated in an air-bath orbital shaker (Nova Etica, model 501/1D) with temperature controlled within 1 K At scheduled time intervals, 2.0 ml was collected from the solution and immediately replenished with pure solvent to maintain the original volume.

2.3. Mathematical modeling

The development of computer technology has enabled the use of numerical techniques to find solutions to engineering and physics problems. From the engineering perspective, the numerical tool is suitable and reliable when it makes use of a numerical method which can correctly solve the differential equations and a mathematical model which is known to faithfully represent the physical phenomenon [8]. In the past 50 years, the mathematical modeling of the diffusion and release of active principles has been used to model systems, from the simple to the complex, to predict the global release behavior [9].

The mathematical modeling carried out in this study involved four types of analysis: the modeling of a matrix where the diffusion coefficient and the mass transfer coefficient are the main parameters of the mass transfer process; the modeling of a solid matrix which dissolves over time, with no change in the volume; the semi-empirical models for the release of the active principles; and the analytical model for Fick's second law.

2.3.1. Modeling of a matrix where the diffusion coefficient and mass transfer coefficient are the main parameters of the mass transfer process

This model considers a sphere, of constant volume, in a bath with agitation kept at a constant temperature. The active compound is released from the interior of the sphere, through pores, and it diffuses to the surface and encounters external resistance to mass transfer. In some situations the external medium (medium 2) influences what happens in medium 1. On considering this influence, an associated resistance, which differs from that of medium 1, is assumed [10] (Fig. 1). In the development of the model the following hypotheses are considered:

i) Matrix-type microcapsule.
ii) No concentration gradient within the agitated reactor (medium 2).
iii) Transient regime: with a variation in the concentration over time in both media (1 and 2).
iv) Constant temperature, pressure and agitation.

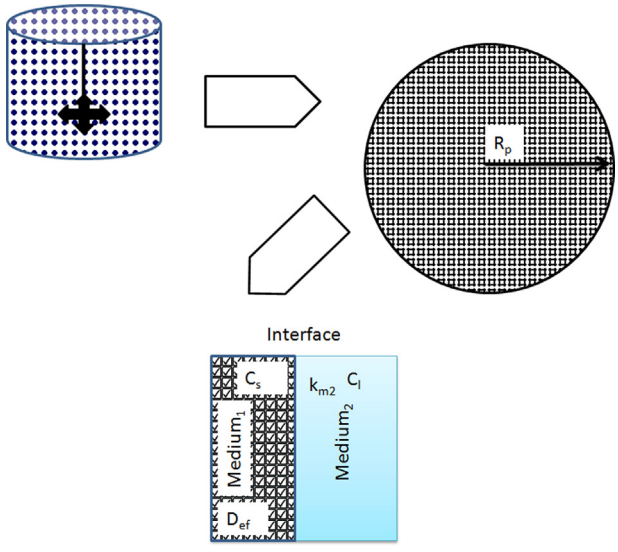

Fig. 1. Scheme of the modeling carried out for a matrix with external resistance to mass transfer.

v) The particle is modeled as a sphere.
vi) The mass transfer flow is unidimensional in r.
vii) The resistance to mass transfer within the particle ($1/D_{pol}$) is fitted to the experimental model.
viii) There is external resistance to mass transfer, related to the transfer coefficient (k_{m2}).
ix) There is no chemical reaction.

In order to calculate the D_{AB} a correlation based on the Stokes-Einstein relation is used, which is known as the Wilke-Chang equation [11]:

$$D_{AB}=\frac{7,\,4x10^{-8}(\phi M_B)^{1/2}T}{\mu_B V_{b_A}^{0.6}} \tag{1}$$

where T is the temperature, μ_B is the dynamic molecular viscosity of the medium, M_B is the molecular weight of B, V_b is the molar volume at the normal boiling temperature and ϕ is the parameter associated with the solvent; $\phi=2.6$ (water), $\phi=1.9$ (methanol), $\phi=1.5$ (ethanol) and $\phi=1$ for the rest of the solvents.

The value for k_{m2} can be calculated using an equation correlated to the Sherwood number [12], given by:

$$k_{m2}=\frac{D_{AB}}{R_p}\left(1+0.\,3\,Re^{0.5}\,Sc^{0.33}\right) \tag{2}$$

where Re is the Reynolds number and Sc is the Schmidt number.

The D_{AB} is calculated in relation to the molar fraction through the following equations:

$$D_{AB}=D_{ABWC}\left[1+x_A\frac{\partial \ln \gamma_A}{\partial x_A}\right] \tag{3}$$

$$\ln \gamma_A=V_A\Phi_B^2\left(\delta_A-\delta_B\right)^2 \tag{4}$$

$$\Phi_B=\frac{x_B V_B}{x_A V_A+x_B V_B} \tag{5}$$

where D_{ABWC} is the diffusivity obtained through the Wilke-Chang correction and V is the molecular volume of A or of B, and δ is the solubility of A or of B. These relations are solved using the computer program Mathematica 4, the following analytical equation begin obtained:

$$D_{AB}=D_{ABWC}\left[1+x_A\left(-\frac{2\left(\delta_A-\delta_B\right)^2V_A\left(V_A-V_B\right)V_B^2\left(1-x_A\right)^2}{RT\left(V_B\left(1-x_A\right)+V_Ax_A\right)^3}-\frac{2\left(\delta_A-\delta_B\right)^2V_AV_B^2(1-x_A)}{RT(V_B\left(1-x_A\right)+V_Ax_A)^2}\right)\right] \tag{6}$$

2.3.2. Mass balance of the solid phase

The balance of the active principle i (for example, betacarotene), will be determined for a control volume defined as a sphere of radius R_p (Fig. 2).

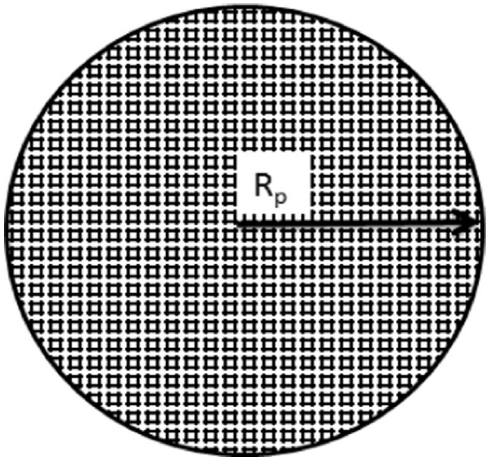

Fig. 2. Scheme of the modeling of the microsphere.

The equation of conservation of chemical species A in terms of mass, in spherical coordinates, adopting the hypotheses previously assumed, is given by:

$$\frac{\partial C_A}{\partial t} = D_{pol}\left[\frac{\partial^2 C_A}{\partial r^2} + \frac{2}{r}\frac{\partial C_A}{\partial r}\right] \tag{7}$$

Eq. (7) is also known as Fick's second law and this is the equation which will be solved computationally for the solid phase in this study. The boundary conditions for the problem are as follows:

Initial condition.

$t = 0;\ 0 \leq r \leq R_p,\ C_A = C_{Ai}$; (for any point within the sphere at the initial time the concentration is the initial concentration of the active principle).

Boundary conditions.

A) $t > 0;\ r = 0$, applying the limit with r tending toward zero in Eq. (7) we have

$$\frac{\partial C_A}{\partial t} = 3D_{pol}\left[\frac{\partial^2 C_A}{\partial r^2}\right] \tag{8}$$

This equation is solved taking in account that $C_{A0} = C_{A2}$.

B) $t > 0;\ r = R_p$, we have $\frac{\partial C_A}{\partial r} = \frac{k_{m2}}{D_{pol} Kp}(C_A^* - C_{AR_p})$; where k_{m2} is the mass transfer coefficient for the external medium, D_{pol} is the diffusivity of the polymer, Kp is the partition coefficient obtained for a linear relation between the equilibrium concentration in the solid phase and the concentration in the liquid phase, C_A^* is the equilibrium concentration and C_{AR_p} is the concentration of A at the particle surface.

2.3.3. Mass balance of the liquid phase

The mass balance as a function of the concentration of the active principle in the solid phase and in the liquid phase (bulk) can be expressed by:

$$V_S\frac{dC_A}{dt} = -V\frac{dC_{Al}}{dt} \tag{9}$$

where V_S is the volume of solid phase in the reactor and V is the volume of liquid phase in the reactor. Eq. (9) can be solved analytically, by assuming that initially the liquid phase is free of the active principle:

$$C_{Al} = \frac{V_S}{V}(C_{Ai} - C_A) \tag{10}$$

2.3.4. Modeling of a solid matrix which dissolves over time, with no change in the volume

The model for a solid matrix which dissolves over time, with no change in the volume, is described below [13]. Fig. 3 shows the scheme for the problem.

In this model it was assumed that:

i) Dissolution was the controlled-release mechanism.
ii) There was a homogeneous distribution of the active principle in the matrix throughout the process.
iii) The concentration varies over time in medium 1 and in medium 2 (transient regime).
iv) The drive force which directs the dissolution is the difference between the concentration of the solid active principle and the corresponding equilibrium concentration in the liquid phase.

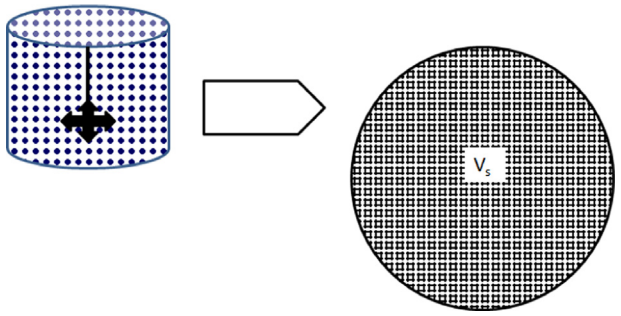

Fig. 3. Scheme for the modeling of the microsphere.

The linear driving force equation for this situation is written as:

$$-\frac{dC_A}{dt}=k_d(C_A-K_pC_{Al}) \tag{11}$$

2.3.5. Mass balance in the liquid phase

The mass balance as a function of the concentration of active principle in the solid phase and in the liquid phase (bulk) can be expressed by:

$$C_{Al}=\frac{V_S}{V}(C_{Ai}-C_A) \tag{12}$$

It is assumed that initially the concentration of the active principle in the liquid phase is equal to zero.

2.3.6. Semi-empirical models for the release of active principles used in this study

The models which provided the best fitting with the data were:

- Korsmeyer-Peppas
- Biexponential

The Korsmeyer-Peppas model is generally used to analyze the release of active compounds from polymeric microcapsules when the release mechanism is not well understood or when more than one type of release mechanism may be involved. In general, 60% of the releases studied showed a good fit with this model [14].

This model is used to describe the release of the solute when the dominant mechanism is a combination of the diffusion of the active principle (Fickian transport) and Case II transport (non Fickian, controlled by the relaxation of the polymeric chains) [15,16]. In this model, the relation between the release rate and time is:

$$\frac{M_t}{M_\infty}=at^n \tag{13}$$

where the parameter a is a constant which incorporates the structural and geometric characteristics of the microcapsule, n is the release exponent, which indicates the mechanism associated with the release of the active principle and $\frac{M_t}{M_\infty}$ is the fractional release of the active principle.

The equation of biexponential model can be expressed as:

$$C=1-[A\exp(-\alpha t)+B\exp(-\beta t)] \tag{14}$$

where C is the concentration of the active principle released at time t as a fraction, α and β are the kinetic rate constants, A and B are the parameters in which the initial portion of the concentration reflects the contribution of the burst effect and continuous phase release, respectively [17].

The numerical method selected to solve the partial differential equations of the model was that of finite differences and for the linearization of the data to obtain the constants of the semi-empirical models the program MATLAB, with the tool CFTOOL, was used.

2.3.7. Analytical model for the release of active principles used in this study

When the active principle is molecularly dispersed in the matrix or it is rapidly or completely dissolved after the penetration of the solvent in the system, the device is called a monolythic solution [18]. The analytical solution is given by:

$$\frac{M_t}{M_\infty}=1-\frac{6}{\pi^2}\sum_{n=1}^{\infty}\frac{\exp\left(-\frac{Dn^2\pi^2t}{Re^2}\right)}{n^2} \tag{15}$$

where M_t is the concentration of the active principle accumulated over time, M_∞ is the concentration of the active principle accumulated in a time tending toward infinite, Re is the external radius of the sphere, D is the coefficient for the diffusion of the active principle through the system and t is time.

This analytical equation is derived from the solution of Fick's second law of diffusion, and the following hypotheses were assumed in order to obtain it [10,19]:

i) The microcapsules do not swell significantly or erode during the release of the active principle (that is, there is no significant alteration in the matrix carrying the active principal).
ii) The microcapsules are spherical.
iii) The active principle is homogeneously distributed inside the microcapsules (spheres).
iv) The release experiment is carried out under perfect immersion conditions.

Table 1.
Types of microcapsules used in the betacarotene release experiment.

Composition of microcapsule	Nomenclature
Betacarotene: 12 mg/ml and PHBV: 30 mg/ml	A
Betacarotene: 14 mg/ml and PHBV: 30 mg/ml	B
Betacarotene: 16 mg/ml and PHBV: 30 mg/ml	C
Betacarotene: 30 mg/ml and PHBV: 30 mg/ml	D

v) The resistance to mass transfer due to the boundary layer is negligible in comparison with that due to diffusion inside the microcapsule (sphere) (that is, the release of the active principle is controlled mainly by its diffusion through the microcapsule).
vi) The dissolution of the active principle is rapid and complete after its exposure to the solvent.
vii) The diffusion coefficient is constant regardless of time or the position within the microcapsule.

3. Results

The experimental data used in this study have been reported in the literature [7,20] and were obtained in studies on the release of betacarotene from microcapsules with four different compositions, using anhydrous ethanol as a solvent. A mathematical model which is mechanistically realistic must be based on a detailed physico-chemical characterization carried out before and after exposure to the release medium [21]. The different compositions of the microcapsules can be seen in Table 1.

The simulated data for the anhydrous ethanol and betacarotene were obtained using the simulation parameters shown in Table 2.

Table 3 shows the physico-chemical parameters for the betacarotene and anhydrous ethanol. The numerical results are given in Figs. 4–7, for the experiments A, B, C and D, respectively in Table 4 are reported the parameters used in the models studied.

After the numerical data had been obtained, statistical analysis was carried out to identify the correlation between the experimental and the fitted data. The results obtained in the *F* test are reported in Table 5, for experimente A.

The results obtained using the models investigated in this study, for experiment A, are shown in Fig. 4.

It can be observed from the experimental results that the release of the active principle from this microcapsule on using a certain solvent was close to 50% at equilibrium. The analysis based on the F test verified that the semi-empirical models gave values closer to 1 and the same was observed for R^2, which indicates that these models provided a better fit with the experimental data. On the other hand, on observing the behavior of the curves it can be concluded that the LDF and CDMASSA models gave a better prediction of the phenomenological behavior of the controlled release. It can be considered that the release process is biphasic, with an initial fast release which later remains constant, as observed in the experimental data. The results obtained with the semi-empirical models showed an increase over time in the fraction of the active principle released, with no plateau being reached. In both analyses the poorest fit was obtained for the analytical model.

Statistical analysis was carried out to compare the numerical data obtained in this study with the experimental data. Table 6 shows the results obtained in the F test and those for R^2 for experiment B.

Fig. 5 reports the results obtained with the use of the models evaluated in this study.

From an analysis based on the F test and R^2, it can be concluded that the models provided good results. The analytical model did not show a good fit in the *F* test but it did give a good result for R^2. Only the LDF model gave a low R^2 value. Based on the experimental data for the release of the active principle, for this microcapsule and solvent, the release was close to 80% when the compound reached equilibrium. It was observed that the release behavior was slightly different for each numerical model used. The semi-empirical models showed increasing release without the presence of a biphasic system while for the CDMASSA and LDF models a biphasic system was observed. The only difference found between the simulations obtained using the CDMASSA and the LDF models was that before reaching equilibrium the release was faster for the LDF model and for the CDMASSA model it was slower, thus better representing numerically the controlled release, as can be observed in Fig. 5.

After the numerical data had been obtained statistical analysis was carried out to identify the correlation between the experimental and fitted data. The results obtained applying the F test are shown in Table 7, for experiment C.

Table 2.
Physico-chemical parameters for betacarotene and anhydrous ethanol.

Parameter	Molar mass (mg/mol)	Solubility ($cal^{1/2}/cm^{3/2}$)	Molar volume (cm^3/mol)	Viscosity (g/cm s)	Specific mass (g/cm^3)
Betacarotene	536,870	8.71	799.2	X	X
Anhydrous ethanol	46,060	12.7	58.5	0.012	0.789

Table 3.
Physico-chemical parameters for betacarotene and anhydrous ethanol.

Parameter	V (ml)	T (K)	D_{AB} (cm^2/s)	Kp	C_0 (mg/ml)	Ceq (mg/ml)	V/Vs
Exp. A	70	313.15	3.056×10^{-6}	379.17	1.315	0.728	305.81
Exp. B	60	313.15	3.056×10^{-6}	96.97	2.6818	0.5721	357.14
Exp. C	60	313.15	3.056×10^{-6}	52.62	4.496	0.5252	400
Exp. D	60	313.15	3.056×10^{-6}	1006.89	16.224	12.425	307.69

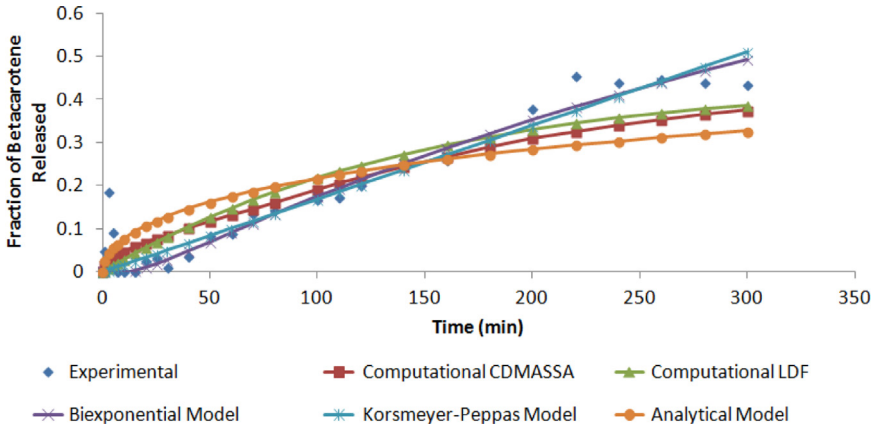

Fig. 4. Simulations using the different models for experiment A (Betacarotene: 12 mg/ml and PHBV: 30 mg/ml and the solvent anhydrous ethanol).

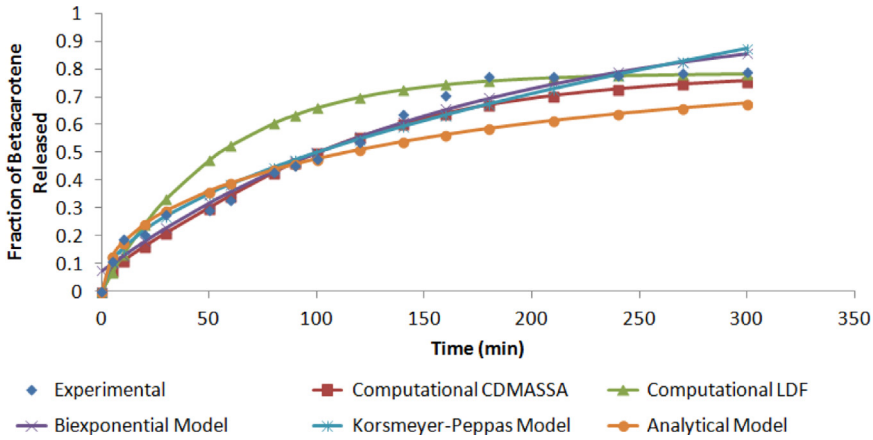

Fig. 5. Simulations using the different models for experiment B (Betacarotene: 14 mg/ml and PHBV: 30 mg/ml and solvent anhydrous ethanol).

The results obtained with the models used in this study can be observed in Fig. 6.

On analyzing the results obtained for the F test applied to the numerical data it can be concluded that the fitted semi-empirical models had values closer to 1, which indicates that they provided a better fit to the experimental data, but according to the R^2 values the CDMASSA appears to be the most suitable model. It can also be observed from the experimental data that the release of the active principle from the microcapsules in this solvent reach equilibrium at close to 90%. The CDMASSA, LDF and biexponential models reached equilibrium, CDMASSA and LDF being the most suitable for the experimental data, which indicates a good phenomenological fit for a system with fast release and a constant final release. This behavior does not occur with the Korsmeyer-Peppas model, where the numerical results show an increase in the release of the active principle without reaching equilibrium, as shown in Fig. 6.

After the numerical data had been obtained statistical analysis was carried out to identify a correlation between the experimental and fitted data. The results obtained applying the F test are shown in Table 8, for experiment D.

The results obtained with the models used in this study can be observed in Fig. 7.

On analyzing the results obtained for the F test and R^2 based on the numerical data it can be concluded that the fitted models had values closer to 1, which indicates that they provided a good fit to the experimental data, with the exception of the analytical model which had an F value much higher than 1. It can be observed that the release of the active principle on reaching equilibrium was close to 25%.

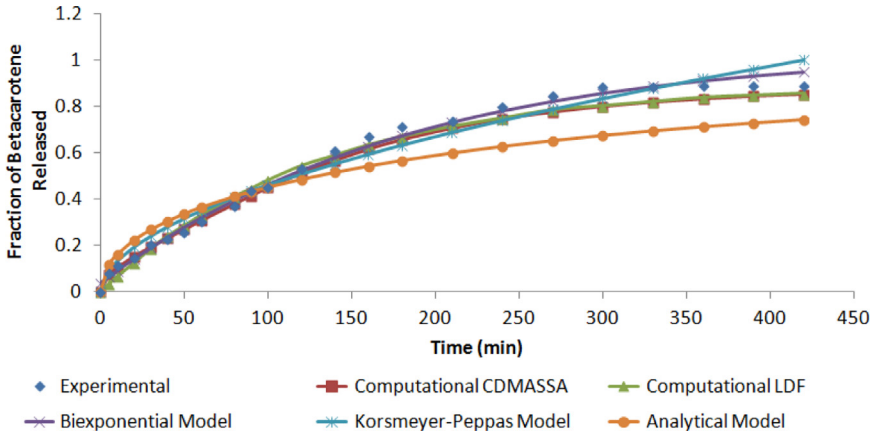

Fig. 6. Simulation using the different models for experiment C (Betacarotene: 16 mg/ml and PHBV: 30 mg/ml and solvent anhydrous ethanol).

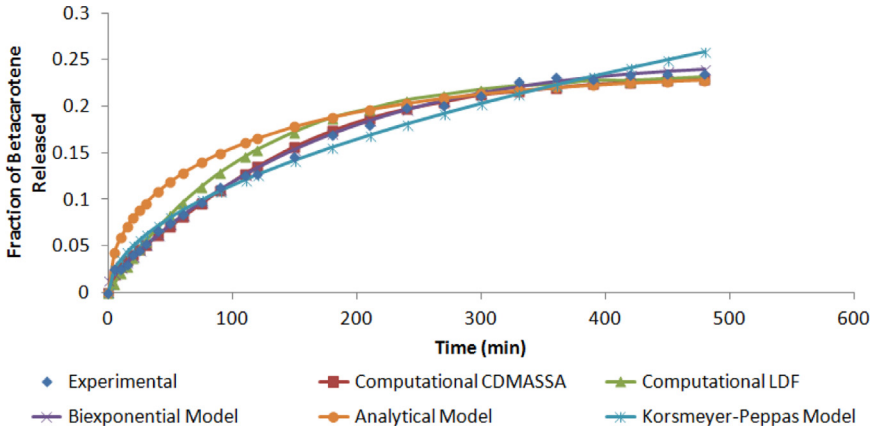

Fig. 7. Simulation using the different models for experiment D (Betacarotene: 30 mg/ml and PHBV: 30 mg/ml and solvent anhydrous ethanol).

Table 4.
Parameters used in the models studied.

Parameter	D_{pol} (cm^2/s)	v_∞ (cm/s)	R_P (cm)	Re	Sc	D_{pol} Analytical (cm^2/s)
Exp. A	3.4×10^{-14}	41.86	5.5×10^{-5}	0.363	4.15×10^{3}	1.47×10^{-14}
Exp. B	5.9×10^{-14}	41.86	5.5×10^{-5}	0.363	4.15×10^{3}	2.5×10^{-14}
Exp. C	4.3×10^{-14}	41.86	5.5×10^{-5}	0.363	4.15×10^{3}	1.6×10^{-14}
Exp. D	4.3×10^{-14}	41.86	5.5×10^{-5}	0.363	4.15×10^{3}	3.17×10^{-14}

Table 5.
Results for F test and R^2 for the models studied in case A (Betacarotene: 12 mg/ml and PHBV: 30 mg/ml and the solvent anhydrous ethanol).

Model studied	F test results	R^2
CDMASSA	1.73	0.88
LDF	1.41	0.85
Biexponential	0.90	0.927
Korsmeyer-Peppas	0.97	0.914
Analytical	2.63	0.77

The parameters for each experiment obtained through the numerical solution of the models, which are shown in Table 9, were the mass transfer coefficient k_{m2} and the diffusivity of the chemical species in the polymer obtained with the CDMASSA and analytical models. The dissolution rate k_d was obtained with the LDF model. The fitting parameters were obtained with the semi-empirical models.

Table 6.
Results for F test and R^2 for the models studied for case B (Betacarotene: 14 mg/ml and PHBV: 30 mg/ml and the solvent anhydrous ethanol).

Model studied	F test results	R^2
CDMASSA	1.07	0.98
LDF	0.94	0.89
Biexponential	1.00	0.97
Korsmeyer-Peppas	1.03	0.97
Analytical	1.76	0.95

Table 7.
Results for the F test and R^2 for the models studied for case C (Betacarotene: 16 mg/ml and PHBV: 30 mg/ml and solvent anhyrous ethanol).

Model studied	F test result	R^2
CDMASSA	1.18	1.00
LDF	1.13	0.99
Biexponential	0.99	0.99
Korsmeyer-Peppas	1.08	0.97
Analytical	2.11	0.97

Table 8.
Results for F test and R^2 for the models studied for case C (Betacarotene: 30 mg/ml and PHBV: 30 mg/ml and the solvent anhydrous ethanol).

Model studied	F test result	R^2
CDMASSA	1.03	0.99
LDF	0.97	0.98
Biexponential	1.00	1.00
Korsmeyer-Peppas	1.07	0.98
Analytical	1.48	0.96

Table 9.
Data obtained with the models for experiments A, B, C and D.

Experiments										
A	CDMASSA		LDF	Biexponential				Korsmeyer-Peppas		Analytical
	k_{m2} (cm/s)	D_{pol} (cm^2/s)	k_d (/s)	A	B	α (/s)	β (/s)	a ($/s^n$)	n	D_{pol} (cm^2/s)
	0.21	3.40×10^{-14}	5×10^{-5}	-2.31×10^{-5}	0.8237	7.43	0.2339	5.98×10^{-5}	1.007	1.47×10^{-14}
B	CDMASSA		LDF	Biexponential				Korsmeyer-Peppas		Analytical
	k_{m2} (cm/s)	D_{pol} (cm^2/s)	k_d (/s)	A	B	α (/s)	β (/s)	a ($/s^n$)	n	D_{pol} (cm^2/s)
	0.21	5.90×10^{-14}	2.4×10^{-4}	−4.761	5.217	0.5196	0.5252	0.007591	0.5085	2.50×10^{-14}
C	CDMASSA		LDF	Biexponential				Korsmeyer-Peppas		Analytical
	k_{m2} (cm/s)	D_{pol} (cm^2/s)	k_d (/s)	A	B	α (/s)	β (/s)	a ($/s^n$)	n	D_{pol} (cm^2/s)
	0.21	4.30×10^{-14}	1.15×10^{-4}	−21.48	21.86	0.5259	0.5313	0.004682	0.5409	1.60×10^{-14}
D	CDMASSA		LDF	Biexponential				Korsmeyer-Peppas		Analytical
	k_{m2} (cm/s)	D_{pol} (cm^2/s)	k_d (/s)	A	B	α (/s)	β (/s)	a ($/s^n$)	n	D_{pol} (cm^2/s)
	0.21	4.30×10^{-14}	3.50×10^{-4}	0.1167	0.7181	0.8018	−0.01296	0.0055	0.51	3.17×10^{-14}

A total of 14 different semi-empirical models were fitted, but the biexponential model showed the best fit for these experimental data. Thus, this model is presented herein. The Korsmeyer-Peppas model is also presented since its fitting can represent the phenomenology of the controlled release.

On observing the F test results for experiment A it can be concluded that the models studied did not provide a good fit for this particular dataset. In the case of the Korsmeyer-Peppas model the constant n had a value of > 0.85, which indicates a non-Fickian transport mechanism, controlled by the relaxation of the polymer chains, which characterizes the deterioration of the microcapsules.

The F test results for experiment B showed a very good fitting of the models to the experimental data. In the case of the Korsmeyer-Peppas model the constant n had a value of between 0.43 and 0.85, which indicates an anomalous diffusion (non-Fickian) transport mechanism, involving both diffusion and relaxation (erosion).

For experiment C, the F test results indicated that the semi-empirical models provided the best fit with the experimental data. In the case of the Korsmeyer-Peppas model, the constant n had a value between 0.43 and 0.85, once again indicating an anomalous diffusion (non-Fickian) transport mechanism, involving both diffusion and relaxation (erosion).

The F test results for experiment D indicated good fits for the models studied to the experimental data. As observed for the experiments B and C, in the case of the Korsmeyer-Peppas model, the constant n had a value between 0.43 and 0.85, indicating an anomalous diffusion (non-Fickian) transport mechanism, involving both diffusion and relaxation (erosion).

The average polymeric diffusivity in relation to the fitting of the CDMASSA model was around 4.4×10^{-14} cm^2/s for the polymer PHBV in a solution of anhydrous ethanol with the diffusion of betacarotene and for the analytical model it was 2.18×10^{-14} cm^2/s. The dissolution rate, which was obtained through the fitting of the LDF model, showed an average of around 1.8×10^{-4}/s for PHBV in a solution of anhydrous ethanol with the dissolution of betacarotene.

The fraction of active principle released before reaching equilibrium differed for each microcapsule studied, indicating that the composition of the microcapsules and the method used to obtain them influenced the amount of active principle released at equilibrium. The fractions released at equilibrium varied between 25% and 95%, indicating that the compositional variability of the microcapsules was very high in these experiments.

4. Conclusions

The data obtained in the simulations indicate that the models studied are able to adequately represent the experimental data analyzed, demonstrating that in relation to the selection of the models, when the diffusion is of Fickian origin the LDF and semi-empirical models were suitable for the description of the experimental data. In most cases, the best fits with the experimental data were obtained using the semi-empirical models, but this was to be expected since these are generally equations fitted to a curve for the specific experimental conditions rather than a set of equations constructed phenomenologically, as in the case of the CDMASSA and analytical models and, in a more simple way, the LDF.

The tests with the PHBV showed good results, indicating that the models used provided a good fit with experimental results available in the literature.

In continuation of this research, a study on different polymeric structures obtained applying the respective procedures will be carried out, since the morphological and system-particle-solvent characteristics strongly influence the experimental results, mainly the fraction released at equilibrium and the time required to reach these levels of release.

References

[1] T.D. Knab, S.R. Little, R.S. Parker, A systems approach to modeling drug release from polymer microspheres to accelerate in vitro to in vivo translation, J. Controll. Release 211 (2015) 74–84, http://dx.doi.org/10.1016/j.jconrel.2015.04.045.

[2] H. Li, J. Chang, Preparation, characterization and in vitro release of gentamicin from PHBV/wollastonite composite microspheres, J. Controll. Release 107 (2005) 463–473, http://dx.doi.org/10.1016/j.jconrel.2005.05.019.

[3] N. Duhem, F. Danhier, V. Préat, Vitamin E-based nanomedicines for anti-cancer drug delivery, J. Controll. Release 182 (2014) 33–44, http://dx.doi.org/10.1016/j.jconrel.2014.03.009.

[4] A. Zabara, R. Mezzenga, Controlling molecular transport and sustained drug release in lipid-based liquid crystalline mesophases, J. Controll. Release 188 (2014) 31–43, http://dx.doi.org/10.1016/j.jconrel.2014.05.052.

[5] I. Martiel, N. Baumann, J.J. Vallooran, J. Bergfreund, L. Sagalowicz, R. Mezzenga, Oil and drug control the release rate from lyotropic liquid crystals, J. Controll. Release 204 (2015) 78–84, http://dx.doi.org/10.1016/j.jconrel.2015.02.034.

[6] J.R. Weiser, W.M. Saltzman, Controlled release for local delivery of drugs: barriers and models, J. Controll. Release 190 (2014) 664–673, http://dx.doi.org/10.1016/j.jconrel.2014.04.048.

[7] W.L. Priamo, A.M. de Cezaro, S.C. Benetti, J.V. Oliveira, S.R.S. Ferreira, In vitro release profiles of β-carotene encapsulated in PHBV by means of supercritical carbon dioxide micronization technique, J. Supercrit. Fluids 56 (2011) 137–143, http://dx.doi.org/10.1016/j.supflu.2010.12.013.

[8] S.V. Patankar, Numerical Heat Transfer and Fluid Flow, Hemisphere Publishing Corporation, New York, http://scholar.google.com/scholar?hl=en&btnG=Search&q=intitle:Numerical+heat+transfer+and+fluid+flow#0.

[9] N. a Peppas, B. Narasimhan, Mathematical models in drug delivery: how modeling has shaped the way we design new drug delivery systems, J. Controll. Release 190 (2014) 75–81, http://dx.doi.org/10.1016/j.jconrel.2014.06.041.

[10] E. Cussler, Diffusion: Mass Transfer in Fluid Systems, 3rd ed. Cambridge University Press, Cambridge, 2009 (accessed 10.10.15) http://medcontent.metapress.com/index/A65RM03P4874243N.pdf.

[11] C.R. Wilke, P. Chang, Correlation of diffusion coefficients in dilute solutions, AIChE J. 1 (1955) 264–270, http://dx.doi.org/10.1002/aic.690010222.

[12] R.B. Bird, W.E. Stewart, E.N. Lightfoot, Transport Phenomena, John Wiley & Sons, New York (2007), http://dx.doi.org/10.1051/jp4:20020462.

[13] M. Polakovič, T. Görner, R. Gref, E. Dellacherie, Lidocaine loaded biodegradable nanospheres: II. Modelling of drug release, J. Controll. Release 60 (1999) 169–177, http://www.sciencedirect.com/science/article/pii/S0168365999000127. (accessed 26.10.14).

[14] N. Peppas, J. Sahlin, A simple equation for the description of solute release. III. Coupling of diffusion and relaxation, Int. J. Pharm. 57 (1989) 169–172. (accessed 16.1.15), http://www.sciencedirect.com/science/article/pii/0378517389903062.

[15] P.L. Ritger, N.A. Peppas, A simple equation for description of solute release I. Fickian and non-fickian release from non-swellable devices in the form of slabs, spheres, cylinders or discs, J. Controll. Release 5 (1987) 23–36.

[16] P.L. Ritger, N.A. Peppas, A simple equation for description of solute release II. Fickian and anomalous release from swellable devices, J. Controll. Release 5 (1987) 37–42.

[17] F.S. Poletto, E. Jäger, M.I. Ré, S.S. Guterres, A.R. Pohlmann, Rate-modulating PHBHV/PCL microparticles containing weak acid model drugs, Int. J. Pharm. 345 (2007) 70–80, http://dx.doi.org/10.1016/j.ijpharm.2007.05.040.

[18] J. Siepmann, F. Siepmann, Modeling of diffusion controlled drug delivery, J. Controll. Release 161 (2012) 351–362, http://dx.doi.org/10.1016/j.jconrel.2011.10.006.

[19] J. Crank, The Mathematics of Diffusion, 2nd ed. Oxford University Press, Bristol. 1975, http://books.google.com/books?hl=en&lr=&id=eHANhZwVouYC&oi=fnd&pg=PA1&dq=The+Mathematic+of+Diffusion&ots=fy-4y-jlOW&sig=7bUh2HpsFuO4NpDhsyIGWDlulF0. (accessed 10.10.15).

[20] W.L. Priamo, A.M. de Cezaro, S.R.S. Ferreira, J.V. Oliveira, Precipitation and encapsulation of β-carotene in PHBV using carbon dioxide as anti-solvent, J. Supercrit. Fluids 54 (2010) 103–109, http://dx.doi.org/10.1016/j.supflu.2010.02.013.

[21] C. Velghe, Y. Rosiaux, D. Marchaud, J. Siepmann, F. Siepmann, In silico simulation of niacin release from lipid tablets: theoretical predictions and independent experiments, J. Controll. Release 175 (2014) 63–71, http://dx.doi.org/10.1016/j.jconrel.2013.12.010.